

This document contains a post-print version of the paper

## Modeling of a permanent magnet synchronous machine with internal magnets using magnetic equivalent circuits

authored by **W. Kemmetmüller, D. Faustner, and A. Kugi**  
and published in *IEEE Transactions on Magnetics*.

---

The content of this post-print version is identical to the published paper but without the publisher's final layout or copy editing. Please, scroll down for the article.

---

### Cite this article as:

W. Kemmetmüller, D. Faustner, and A. Kugi, "Modeling of a permanent magnet synchronous machine with internal magnets using magnetic equivalent circuits", *IEEE Transactions on Magnetics*, vol. 50, no. 6, 2014. DOI: [10.1109/TMAG.2014.2299238](https://doi.org/10.1109/TMAG.2014.2299238)

---

### BibTeX entry:

```
% This file was created with JabRef 2.9.2.  
% Encoding: Cp1252
```

```
@ARTICLE{acinpaper,  
  author = {Kemmetmüller, W. and Faustner, D. and Kugi, A.},  
  title = {Modeling of a permanent magnet synchronous machine with internal  
          magnets using magnetic equivalent circuits},  
  journal = {IEEE Transactions on Magnetics},  
  year = {2014},  
  volume = {50},  
  number = {6},  
  part = {2},  
  doi = {10.1109/TMAG.2014.2299238}  
}
```

---

### Link to original paper:

<http://dx.doi.org/10.1109/TMAG.2014.2299238>

---

### Read more ACIN papers or get this document:

<http://www.acin.tuwien.ac.at/literature>

---

### Contact:

Automation and Control Institute (ACIN)  
Vienna University of Technology  
Gusshausstrasse 27-29/E376  
1040 Vienna, Austria

Internet: [www.acin.tuwien.ac.at](http://www.acin.tuwien.ac.at)  
E-mail: [office@acin.tuwien.ac.at](mailto:office@acin.tuwien.ac.at)  
Phone: +43 1 58801 37601  
Fax: +43 1 58801 37699

---

### Copyright notice:

© 2014 IEEE. Personal use of this material is permitted. Permission from IEEE must be obtained for all other uses, in any current or future media, including reprinting/republishing this material for advertising or promotional purposes, creating new collective works, for resale or redistribution to servers or lists, or reuse of any copyrighted component of this work in other works.

# Modeling of a permanent magnet synchronous machine with internal magnets using magnetic equivalent circuits

Wolfgang Kemmetmüller<sup>1</sup> *Member, IEEE*, David Faustner<sup>1</sup>, and Andreas Kugi<sup>1</sup> *Member, IEEE*

<sup>1</sup>Automation and Control Institute, Vienna University of Technology, Vienna, Austria

The design of control strategies for permanent magnet synchronous machines (PSM) is almost exclusively based on classical dq0-models. These models are, however, not able to systematically describe saturation or non-homogenous air gap geometries typically occurring in PSM. This paper deals with a framework for the mathematical modeling of PSM based on magnetic equivalent circuits. Different to existing works, the model equations are derived by means of graph theory allowing for a systematic choice of a minimal set of state variables of the model and a systematic consideration of the electrical connection of the coils of the motor. The resulting model is calibrated and verified by means of measurement results. Finally, a magnetically linear and a dq0-model are derived and their performance is compared with the nonlinear model and measurement results.

*Index Terms*—magnetic equivalent circuit, electric motor, permanent magnet motors

## I. INTRODUCTION

PERMANENT magnet synchronous motors (PSM) are widely used in many technical applications. Numerous papers and books dealing with the design of PSM have been published in recent years, see, e.g., [1], [2], [3], [4], [5], [6], [7]. The mathematical models proposed in these papers range from finite element analysis over reluctance models to classical dq0-models. Finite element (FE) models exhibit a high accuracy for the calculated magnetic fields and allow for an exact consideration even of complex geometries of the motor, see, e.g., [5], [6], [7], [8], [9], [10]. Due to their high (numeric) complexity, these models are, however, hardly suitable for dynamical simulations and a controller design.

The design of control strategies for PSM is typically based on classical dq0-models, which, in their original form, assume a homogenous air gap and unsaturated iron cores, see, e.g., [11], [12], [13], [14], [15], [16], [17], [18]. Many modern designs of PSM (including e.g. PSM with internal magnets) exhibit considerable saturation and non-sinusoidal fluxes in the coils. To cope with these effects, extensions of dq0-models have been reported in literature, which are all based on a heuristic approach and are limited to a very specific motor design, see, e.g., [16], [17], [18]. In most cases, these models are not able to accurately describe the motor behavior in all operating conditions.

Magnetic equivalent circuits have become very popular for the design and the (dynamical) simulation of PSM in the recent years, see, e.g., [1], [2], [19], [20], [21], [22], [23], [24], [25], [26], [27], [28], [29], [30], [31], [32], [33], [34], [35]. This is due to the significantly reduced complexity in comparison to FE models and their capability to systematically describe saturation and non-homogenous air gap geometries. The accuracy and complexity of reluctance models can be easily controlled by means of the choice of the reluctance network. While reluctance networks with a rather high com-

plexity are necessary to accurately describe field profiles in the motor, models of significantly reduced complexity already represent the behavior with respect to the torque, currents and voltages of the motor in sufficient detail. Thus, models based on adequately chosen reluctance models promise to be a good basis for dynamical simulations and the (nonlinear) controller design.

In this paper, a framework for the systematic derivation of a state-space model with a minimum number of nonlinear equations and state variables is presented. The main purpose of the derived model is to provide a state-space representation for advanced model-based control strategies and thus to reproduce the dynamic input-to-output behavior of the motor in an accurate manner. The framework developed here is universal, it is applied here to a specific internal magnet PSM that exhibits both large cogging torque and saturation. Section II presents the considered model and a complete reluctance model of the motor. To obtain a minimal set of (nonlinear) equations that describe the reluctance network, a method based on graph theory is proposed. This method, well known from electrical networks, see, e.g. [36], [37], [38] is adjusted to the analysis of magnetic networks. Subsequently, the description of the electrical connection of the coils and the choice of a suitable set of state variables for the dynamical system is outlined. It should be noted that the framework presented in this section can be applied to any PSM. Section III is concerned with a reduced model based on findings of simulation results of the complete model. Section IV shows the systematic calibration of the reduced model and a comparison with measurement results. Starting from the nonlinear model, a magnetically linear model and a classical dq0-model are systematically derived in Section V. Finally, the results of the nonlinear model, the magnetically linear model and the dq0-model are compared with measurement results.

## II. CONSIDERED MOTOR AND COMPLETE MODEL

The motor considered in this paper is a permanent magnet synchronous motor with internal magnets. It comprises 12

Manuscript received September 26, 2013; revised ??, 2013. Corresponding author: W. Kemmetmüller (email: kemmetmueller@acin.tuwien.ac.at).



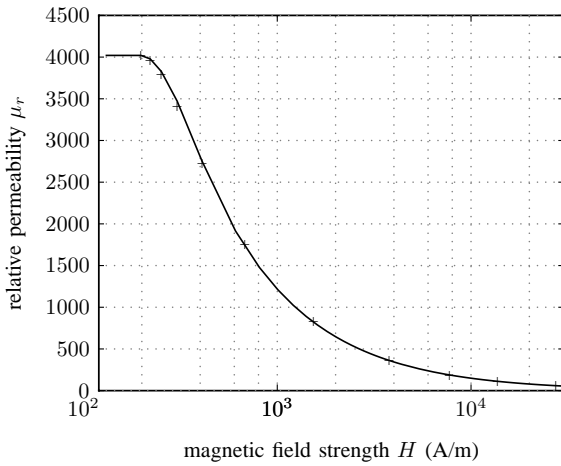


Fig. 3. Relative permeability  $\mu_r$  of the core material M800-50A.

by

$$G_{bjk}(u_{bjk}) = \frac{A_{bc}\mu_0\mu_r\left(\frac{|u_{bjk}|}{l_{bc}}\right)}{l_{bc}}, \quad jk \in \{11, 12, 21, 22\}, \quad (4)$$

with the area  $A_{bc}$ , the length  $l_{bc}$  and the magnetomotive force  $u_{bjk}$ . The permeances of the radial bars read as

$$G_{bj}(u_{bj}) = \frac{A_{br}\mu_0\mu_r\left(\frac{|u_{bj}|}{l_{br}}\right)}{l_{br}}, \quad j = 1, 2. \quad (5)$$

Again,  $A_{br}$  denotes the area,  $l_{br}$  the length and  $u_{brj}$  the magnetomotive force of the radial bar element.

The air gap of the motor is modeled by two types of permeances: the permeances  $G_{ljk}$ ,  $jk \in \{12, 23, 31\}$ , describing the leakage between adjacent stator teeth, and  $G_{ajk}$ ,  $jk \in \{11, 12, 21, 22, 31, 32\}$ , describing the coupling between stator and rotor. The leakage permeances are defined as

$$G_{ljk} = \frac{A_l\mu_0}{l_l}, \quad jk \in \{12, 23, 31\}, \quad (6)$$

with the effective area  $A_l$  and length  $l_l$ . The air gap permeances  $G_{ajk}$  are, of course, functions of the relative rotation  $\varphi$  of the rotor with respect to the stator. A geometric model of these permeances using an approximate air gap geometry is possible but yields inaccurate results due to stray fluxes not covered by the approximate air gap geometry. Therefore, a heuristic approach, as has been proposed in [2], [19], is used to approximate the coupling between the rotor and stator, i.e. the air gap permeance  $G_a$ .

$$G_a(\varphi) = \begin{cases} 0 & -\frac{\pi}{4} \leq \tilde{\varphi} \leq -\delta \\ \frac{G_{a,max}}{2} (1 + \cos(\frac{\pi}{\delta}\tilde{\varphi})) & -\delta < \tilde{\varphi} \leq \delta \\ 0 & \delta < \tilde{\varphi} \leq \frac{\pi}{4} \end{cases} \quad (7)$$

Therein,  $\tilde{\varphi}$  is the relative rotation  $\varphi$  mapped to the interval  $(-\pi/4, \pi/4)$  by means of a modulo operation. Moreover,  $\delta$  is a parameter which can be approximately determined by the geometrical overlap between a permanent magnet and a stator

tooth, and  $G_{a,max}$  is the maximum value at  $\tilde{\varphi} = 0$ . Given  $G_a$  of (7), the air gap permeances between the individual stator teeth and permanent magnets are defined as

$$G_{ajk} = G_a\left(\varphi - \frac{(j-1)\pi}{6} - \frac{(k-1)\pi}{4}\right), \quad (8)$$

with  $j = 1, 2, 3$  and  $k = 1, 2$ .

The NdFeB-magnets exhibit an almost linear behavior in the operating range, which can be modeled in the form of a constant magnetomotive force  $u_{msj}$ ,  $j = 1, 2$  and a linear permeance

$$G_{mj}(u_{mj}) = \frac{A_m\mu_0\mu_{rm}}{l_m}, \quad j = 1, 2, \quad (9)$$

with the constant relative permeability  $\mu_{rm}$ , the effective area  $A_m$  and the length  $l_m$ . Given the coercive field strength  $H_c$  of the magnets, their magnetomotive forces are described by

$$u_{ms1} = -u_{ms2} = -H_cl_m. \quad (10)$$

The stator coils with  $N_c$  turns are modeled by

$$u_{csj} = N_c i_{cj}, \quad j = 1, 2, 3, \quad (11)$$

with  $i_{cj}$  being the electric current through the coil  $j$ .

## B. Balance equations

Two approaches for the derivation of the balance equations (Kirchhoff's node and branch equations) are typically used for magnetic reluctance networks: (i) mesh analysis [33], [34], [35] and (ii) node potential analysis [2], [19], [20], [21], [23], [25], [26], [27], [28]. While a proper choice of meshes, yielding a set of independent equations might be tricky, the node potential analysis automatically guarantees the independence of the resulting equations. Therefore, node potential analysis is typically favored.

In this paper an alternative approach for the systematic derivation of a minimal set of independent equations based on graph theory is proposed. It uses a tree, which connects all nodes of the network without forming any meshes. This approach is well known from electric network analysis, see, e.g., [36], [37], [38], and can be, as will be shown in this paper, directly applied to magnetic permeance networks, see also [29].

The chosen tree has to connect all nodes of the network without forming any meshes. Moreover, all magnetomotive force sources have to be included in the tree, which is always possible for non-degenerated networks. It further turns out to be advantageous to exclude as many air gap permeance from the tree as possible. One possible choice of a tree is given in Fig. 2 by the components depicted in black. The co-tree is then composed of all components which are not part of the tree (depicted gray in Fig. 2). Adding one co-tree element to the tree yields a single mesh.

For the subsequent derivation, it is useful to subdivide the elements of the tree into magnetomotive force sources of the coils (index  $tc$ ), magnetomotive force sources of the permanent magnets (index  $tm$ ) and permeances (linear, nonlinear, angle

dependent, index  $tg$ ). Then, the overall vector of the tree fluxes  $\phi_t = [\phi_{tc}^T, \phi_{tm}^T, \phi_{tg}^T]^T$  is defined by

$$\phi_{tc} = [\phi_{cs1}, \phi_{cs2}, \phi_{cs3}]^T \quad (12a)$$

$$\phi_{tm} = [\phi_{ms1}, \phi_{ms2}]^T \quad (12b)$$

$$\phi_{tg} = [\phi_{s1}, \phi_{s2}, \phi_{s3}, \phi_{s12}, \phi_{s23}, \phi_{b1}, \phi_{b2}, \phi_{r11}, \phi_{r12}, \phi_{r21}, \phi_{m1}, \phi_{m2}, \phi_{a11}]^T. \quad (12c)$$

The vector of the corresponding tree magnetomotive forces  $\mathbf{u}_t$  is defined in an analogous manner.

The co-tree only comprises permeances such that the vector of the co-tree fluxes is given by

$$\phi_c = [\phi_{l12}, \phi_{l23}, \phi_{l31}, \phi_{s31}, \phi_{b11}, \phi_{b12}, \phi_{b21}, \phi_{b22}, \phi_{r22}, \phi_{a12}, \phi_{a21}, \phi_{a22}, \phi_{a31}, \phi_{a32}]^T \quad (13)$$

and the vector of co-tree magnetomotive forces  $\mathbf{u}_c$  is defined in the same way. Now, the following relations between the tree and co-tree fluxes and magnetomotive forces, respectively, can be formulated

$$\phi_t = \mathbf{D}\phi_c \quad (14a)$$

$$\mathbf{u}_c = -\mathbf{D}^T\mathbf{u}_t. \quad (14b)$$

The incidence matrix  $\mathbf{D}$  describes the interconnection of the individual elements of the permeance network and its entries are either  $-1$ ,  $0$  or  $1$ . It can be decomposed into a part  $\mathbf{D}_c$  linking the co-tree fluxes with the tree coil fluxes, a part  $\mathbf{D}_m$  linking the co-tree fluxes with the tree permanent magnet fluxes, and a part  $\mathbf{D}_g$ , which connects the co-tree fluxes with the fluxes of the tree permeances, i.e.  $\mathbf{D}^T = [\mathbf{D}_c^T, \mathbf{D}_m^T, \mathbf{D}_g^T]$ .

The constitutive equations of the permeances can be summarized in the form

$$\phi_{tg} = \mathbf{G}_t\mathbf{u}_{tg} \quad (15a)$$

$$\phi_c = \mathbf{G}_c\mathbf{u}_c, \quad (15b)$$

with the permeance matrices  $\mathbf{G}_t$  and  $\mathbf{G}_c$  of the tree and co-tree, respectively. Note that in general these matrices are functions of the corresponding magnetomotive forces (due to saturation) and the displacement of the rotor, i.e.  $\mathbf{G}_t(\mathbf{u}_{tg}, \varphi)$  and  $\mathbf{G}_c(\mathbf{u}_c, \varphi)$ . For the permeance network of Fig. 2 these matrices read as

$$\mathbf{G}_t = \text{diag}[G_{s1}, G_{s2}, G_{s3}, G_{s12}, G_{s23}, G_{b1}, G_{b2}, G_{r11}, G_{r12}, G_{r21}, G_{m1}, G_{m2}, G_{a11}] \quad (16a)$$

$$\mathbf{G}_c = \text{diag}[G_{l12}, G_{l23}, G_{l31}, G_{s31}, G_{b11}, G_{b12}, G_{b21}, G_{b22}, G_{r22}, G_{a12}, G_{a21}, G_{a22}, G_{a31}, G_{a32}]. \quad (16b)$$

Inserting (15) into (14), we find the following set of equations

$$\begin{bmatrix} \phi_{tc} \\ \phi_{tm} \\ \mathbf{G}_t\mathbf{u}_{tg} \end{bmatrix} = -\mathbf{D}\mathbf{G}_c [\mathbf{D}_c^T, \mathbf{D}_m^T, \mathbf{D}_g^T] \begin{bmatrix} \mathbf{u}_{tc} \\ \mathbf{u}_{tm} \\ \mathbf{u}_{tg} \end{bmatrix}. \quad (17)$$

If it is assumed that the coil currents  $\mathbf{i}_c = [i_{c1}, i_{c2}, i_{c3}]^T$  and thus the magnetomotive forces  $\mathbf{u}_{tc}$  are given, the unknown

variables of (17) are  $\phi_{tm}$  and  $\mathbf{u}_{tg}$ . A simple reformulation of (17) yields

$$\begin{bmatrix} \mathbf{I} & \mathbf{0} & \mathbf{D}_c\mathbf{G}_c\mathbf{D}_g^T \\ \mathbf{0} & \mathbf{I} & \mathbf{D}_m\mathbf{G}_c\mathbf{D}_g^T \\ \mathbf{0} & \mathbf{0} & \mathbf{G}_t + \mathbf{D}_g\mathbf{G}_c\mathbf{D}_g^T \end{bmatrix} \begin{bmatrix} \phi_{tc} \\ \phi_{tm} \\ \mathbf{u}_{tg} \end{bmatrix} = -\mathbf{D}\mathbf{G}_c (\mathbf{D}_c^T\mathbf{u}_{tc} + \mathbf{D}_m^T\mathbf{u}_{tm}) \quad (18)$$

with the identity matrix  $\mathbf{I}$ . It can be easily seen that a set of  $\dim(\mathbf{u}_{tg}) = n = 13$  nonlinear algebraic equations has to be solved for  $\mathbf{u}_{tg}$ . All other quantities of the network can be calculated from simple linear equations. A proof of the existence and uniqueness of a solution of the nonlinear algebraic equations (18) is given in the Appendix A.

### C. Torque equation

Starting from the magnetic co-energy of the permeance network, the electromagnetic torque of the motor is defined as

$$\tau = \frac{1}{2}p \left( \mathbf{u}_{tg}^T \frac{\partial \mathbf{G}_t}{\partial \varphi} \mathbf{u}_{tg} + \mathbf{u}_c^T \frac{\partial \mathbf{G}_c}{\partial \varphi} \mathbf{u}_c \right), \quad (19)$$

with the number  $p$  of pole pairs, see, e.g., [2]. With the help of (14b) this equation can be reformulated in the form

$$\tau = \frac{1}{2}p \left( \mathbf{u}_{tg}^T \frac{\partial \mathbf{G}_t}{\partial \varphi} \mathbf{u}_{tg} + \mathbf{u}_t^T \mathbf{D} \frac{\partial \mathbf{G}_c}{\partial \varphi} \mathbf{D}^T \mathbf{u}_t \right), \quad (20)$$

with  $\mathbf{u}_t^T = [\mathbf{u}_{tc}^T, \mathbf{u}_{tm}^T, \mathbf{u}_{tg}^T]$ .

### D. Voltage equation

The mathematical model (18) and (20) allows for a calculation of the magnetomotive forces, fluxes and the torque for given currents  $\mathbf{i}_c$ . This model is useful for a static analysis of the motor. In a dynamical analysis, however, the coil voltages  $\mathbf{v}_c$  must be used as inputs. This relation is provided by Faraday's law

$$\frac{d\psi_c}{dt} = \mathbf{R}_c\mathbf{i}_c - \mathbf{v}_c, \quad (21)$$

with the flux linkage  $\psi_c = \mathbf{N}_c\phi_{tc}$ , the winding matrix  $\mathbf{N}_c = \text{diag}[N_c, N_c, N_c]$ , the electric resistance matrix  $\mathbf{R}_c = \text{diag}[R_c, R_c, R_c]$  and the electric voltages  $\mathbf{v}_c = [v_{c1}, v_{c2}, v_{c3}]^T$ . Here,  $N_c$  is the number of turns,  $R_c$  the electric resistance and  $v_{cj}$  the voltage of the respective coil  $j = 1, 2, 3$ . Eq. (21) links the fluxes  $\phi_{tc}$  of the coils with their currents  $\mathbf{i}_c$ . Thus, either  $\phi_{tc}$  has to be defined as a function of  $\mathbf{i}_c$  or vice versa. For nonlinear permeance networks, it proves to be advantageous to express the coil currents  $\mathbf{i}_c$  as functions of the fluxes by reformulating (18) in the form

$$\underbrace{\begin{bmatrix} \mathbf{D}_c\mathbf{G}_c\mathbf{D}_c^T & \mathbf{0} & \mathbf{D}_c\mathbf{G}_c\mathbf{D}_g^T \\ \mathbf{D}_m\mathbf{G}_c\mathbf{D}_c^T & \mathbf{I} & \mathbf{D}_m\mathbf{G}_c\mathbf{D}_g^T \\ \mathbf{D}_g\mathbf{G}_c\mathbf{D}_c^T & \mathbf{0} & \mathbf{G}_t + \mathbf{D}_g\mathbf{G}_c\mathbf{D}_g^T \end{bmatrix}}_{\mathbf{K}_1} \underbrace{\begin{bmatrix} \mathbf{u}_{tc} \\ \phi_{tm} \\ \mathbf{u}_{tg} \end{bmatrix}}_{\mathbf{x}} = \underbrace{\begin{bmatrix} \phi_{tc} \\ \mathbf{0} \\ \mathbf{0} \end{bmatrix}}_{\mathbf{M}_1} - \underbrace{\mathbf{D}\mathbf{G}_c\mathbf{D}_m^T\mathbf{u}_{tm}}_{\mathbf{M}_2}. \quad (22)$$

This means that the dynamical model of the motor is given by a set of nonlinear differential-algebraic equations (DAE), i.e. (21) and (22). Now, the following questions arise:

- 1) Do the state variables of (21) represent the minimum number of states or is it possible to reduce the number of states?
- 2) Does the nonlinear set of equations (22) have a unique solution?
- 3) How can the electric interconnection of the coils (e.g. delta or wye connection) be systematically taken into account?

To answer the first two questions consider the matrix  $\mathbf{K}_1$  of (22). Using the results of Appendix A, it turns out that  $\mathbf{K}_1$  is singular if the rows of  $\mathbf{D}_c$  are linearly dependent. Let us assume that  $\mathbf{D}_c \in \mathbb{R}^{m \times n}$ ,  $m < n$  has  $m^\perp$  linear dependent rows. Then, the column space  $\mathcal{D}_c^I = \text{span}(\mathbf{D}_c)$  has dimension  $m - m^\perp$  and the orthogonal complement  $\mathcal{D}_c^\perp = \text{span}(\mathbf{a} \in \mathbb{R}^m | \mathbf{a}^T \mathbf{b} = 0, \forall \mathbf{b} \in \mathcal{D}_c^I)$  has dimension  $m^\perp$ . Let  $\mathbf{D}_c^I$  be a matrix composed of  $m - m^\perp$  independent vectors of  $\mathcal{D}_c^I$  (i.e. the image of  $\mathbf{D}_c$ ) and  $\mathbf{D}_c^\perp$  be composed of  $m^\perp$  independent vectors of  $\mathcal{D}_c^\perp$  (i.e. the kernel of  $\mathbf{D}_c^T$ ). Then,  $(\mathbf{D}_c^\perp)^T \mathbf{D}_c = \mathbf{0}$  holds and the nonsingular matrix

$$\mathbf{T}_1 = \begin{bmatrix} \mathbf{T}_{1c} & \mathbf{0} & \mathbf{0} \\ \mathbf{0} & \mathbf{I} & \mathbf{0} \\ \mathbf{0} & \mathbf{0} & \mathbf{I} \end{bmatrix} \quad (23)$$

with

$$\mathbf{T}_{1c} = \begin{bmatrix} (\mathbf{D}_c^\perp)^T \\ (\mathbf{D}_c^I)^T \end{bmatrix} \quad (24)$$

can be defined. Applying the transformation matrix  $\mathbf{T}_1$  in the form

$$\underbrace{\mathbf{T}_1 \mathbf{K}_1 \mathbf{T}_1^{-1}}_{\mathbf{K}_2} \mathbf{T}_1 \begin{bmatrix} \mathbf{u}_{tc} \\ \phi_{tm} \\ \mathbf{u}_{tg} \end{bmatrix} = -\mathbf{T}_1 \mathbf{M}_1 - \mathbf{T}_1 \mathbf{M}_2 \quad (25)$$

results in a matrix  $\mathbf{K}_2$  with the structure

$$\mathbf{K}_2 = \begin{bmatrix} \mathbf{0} & \mathbf{0} \\ \mathbf{0} & \mathbf{K}_{2r} \end{bmatrix}, \quad (26)$$

where the number of zero rows and columns is  $m^\perp$ . To prove this statement,  $\mathbf{K}_2$  is formulated as

$$\mathbf{K}_2 = \begin{bmatrix} \mathbf{T}_{1c} \mathbf{D}_c \mathbf{G}_c \mathbf{D}_c^T \mathbf{T}_{1c}^{-1} & \mathbf{0} & \mathbf{T}_{1c} \mathbf{D}_c \mathbf{G}_c \mathbf{D}_g^T \\ \mathbf{D}_m \mathbf{G}_c \mathbf{D}_c^T \mathbf{T}_{1c}^{-1} & \mathbf{I} & \mathbf{D}_m \mathbf{G}_c \mathbf{D}_g^T \\ \mathbf{D}_g \mathbf{G}_c \mathbf{D}_c^T \mathbf{T}_{1c}^{-1} & \mathbf{0} & \mathbf{G}_t + \mathbf{D}_g \mathbf{G}_c \mathbf{D}_g^T \end{bmatrix}. \quad (27)$$

It can be seen that the product

$$\mathbf{T}_{1c} \mathbf{D}_c = \begin{bmatrix} \mathbf{0} \\ (\mathbf{D}_c^I)^T \mathbf{D}_c \end{bmatrix} \quad (28)$$

gives  $m^\perp$  zero rows. Of course, the right-hand side multiplication with an arbitrary matrix does not change the zero rows. To prove the zero columns in  $\mathbf{K}_2$ , the product  $\mathbf{D}_c^T \mathbf{T}_{1c}^{-1}$

is analyzed. The matrix  $\mathbf{T}_{1c}$  can be written in the form

$$\mathbf{T}_{1c} = \begin{bmatrix} \mathbf{a}_1^T \\ \vdots \\ \mathbf{a}_{m-m^\perp}^T \\ \mathbf{b}_1^T \\ \vdots \\ \mathbf{b}_{m-m^\perp}^T \end{bmatrix}, \quad (29)$$

where  $\mathbf{a}_j \in \mathcal{D}_c^\perp$  and  $\mathbf{b}_j \in \mathcal{D}_c^I$ . The inverse  $\mathbf{T}_{1c}^{-1} = [\mathbf{v}_1, \dots, \mathbf{v}_{m-m^\perp}, \mathbf{w}_1, \dots, \mathbf{w}_{m-m^\perp}]$  has to meet  $\mathbf{T}_{1c} \mathbf{T}_{1c}^{-1} = \mathbf{I}$  and therefore

$$\mathbf{a}_j^T \mathbf{v}_k = \delta_{jk} \quad \mathbf{a}_j^T \mathbf{w}_k = 0 \quad (30a)$$

$$\mathbf{b}_j^T \mathbf{w}_k = \delta_{jk} \quad \mathbf{b}_j^T \mathbf{v}_k = 0, \quad (30b)$$

with the Kronecker symbol  $\delta_{jk}$ , holds. Obviously, this means that  $\mathbf{v}_j \in \mathcal{D}_c^\perp$  and  $\mathbf{w}_j \in \mathcal{D}_c^I$ . Based on this discussion

$$\mathbf{D}_c^T \mathbf{T}_{1c}^{-1} = [\mathbf{0}, \star] \quad (31)$$

holds, where the number of zero columns is equal to  $m^\perp$  and  $\star$  is a matrix with  $m - m^\perp$  non-zero columns. Thus,  $\mathbf{K}_2$  has  $m^\perp$  zero columns and rows.

The application of  $\mathbf{T}_1$  to the vector of unknowns gives

$$\mathbf{T}_1 \begin{bmatrix} \mathbf{u}_{tc} \\ \phi_{tm} \\ \mathbf{u}_{tg} \end{bmatrix} = \begin{bmatrix} \mathbf{T}_{1c} \mathbf{u}_{tc} \\ \phi_{tm} \\ \mathbf{u}_{tg} \end{bmatrix}, \quad (32)$$

the multiplication of  $\mathbf{M}_1$  with the transformation matrix results in

$$\mathbf{T}_1 \begin{bmatrix} \phi_{tc} \\ \mathbf{0} \\ \mathbf{0} \end{bmatrix} = \begin{bmatrix} \mathbf{T}_{1c} \phi_{tc} \\ \mathbf{0} \\ \mathbf{0} \end{bmatrix} \quad (33)$$

and  $\mathbf{T}_1$  used in combination with  $\mathbf{M}_2$  yields

$$\mathbf{T}_1 \mathbf{D} \mathbf{G}_c \mathbf{D}_g^T \mathbf{u}_{tm} = \begin{bmatrix} \mathbf{T}_{1c} \mathbf{D}_c \\ \mathbf{D}_m \\ \mathbf{D}_g \end{bmatrix} \mathbf{G}_c \mathbf{D}_g^T \mathbf{u}_{tm}, \quad (34)$$

which again has  $m^\perp$  zero rows.

This discussion shows two important results: (i) From (25) with (32) and (24) it can be seen that the part  $(\mathbf{D}_c^\perp)^T \mathbf{u}_{tc}$  of the coil currents cannot be calculated from the permeance network but has to be defined by the electrical connection of the coils. Only the part  $(\mathbf{D}_c^I)^T \mathbf{u}_{tc}$  is determined by the (reduced) set of nonlinear equations

$$\mathbf{K}_{2r} \begin{bmatrix} (\mathbf{D}_c^I)^T \mathbf{u}_{tc} \\ \phi_{tm} \\ \mathbf{u}_{tg} \end{bmatrix} = - \begin{bmatrix} (\mathbf{D}_c^I)^T \phi_{tc} \\ \mathbf{0} \\ \mathbf{0} \end{bmatrix} - \begin{bmatrix} (\mathbf{D}_c^I)^T \mathbf{D}_c \\ \mathbf{D}_m \\ \mathbf{D}_g \end{bmatrix} \mathbf{G}_c \mathbf{D}_g^T \mathbf{u}_{tm}. \quad (35)$$

(ii) Not the entire part of  $\phi_{tc}$  is independent but the components are restricted to fulfill

$$(\mathbf{D}_c^\perp)^T \phi_{tc} = \mathbf{0}. \quad (36)$$

This implies that the set of differential equations (21) for the flux linkage can be reduced to  $m - m^\perp$  differential equations, where  $(\mathbf{D}_c^I)^T \phi_{tc}$  is a possible choice of independent states.

*Remark 1:* To systematically obtain the reduced set of nonlinear equations from the transformed set of equations (25), the reduction matrix  $\mathbf{H}_1$ ,

$$\mathbf{H}_1 = \begin{bmatrix} \mathbf{H}_{1r} & \mathbf{0} & \mathbf{0} \\ \mathbf{0} & \mathbf{I} & \mathbf{0} \\ \mathbf{0} & \mathbf{0} & \mathbf{I} \end{bmatrix}, \quad (37)$$

$\mathbf{H}_1 \mathbf{H}_1^T = \mathbf{I}$  with  $\mathbf{H}_{1r} = [\mathbf{0}, \mathbf{I}] \in \mathbb{R}^{(m-m^\perp) \times m}$ , is introduced. Multiplying (25) with  $\mathbf{H}_1$  from the left side directly yields the reduced equations

$$\underbrace{\mathbf{H}_1 \mathbf{K}_2 \mathbf{H}_1^T}_{\mathbf{K}_{2r}} \begin{bmatrix} \mathbf{H}_{1r} \mathbf{T}_{1c} \mathbf{u}_{tc} \\ \phi_{tm} \\ \mathbf{u}_{tg} \end{bmatrix} = - \begin{bmatrix} \mathbf{H}_{1r} \mathbf{T}_{1c} \phi_{tc} \\ \mathbf{0} \\ \mathbf{0} \end{bmatrix} - \mathbf{H}_1 \mathbf{T}_1 \mathbf{M}_2 \quad (38)$$

with

$$\mathbf{K}_{2r} = \begin{bmatrix} \mathbf{H}_{1r} \mathbf{T}_{1c} \mathbf{D}_c \mathbf{G}_c \mathbf{D}_c^T \mathbf{T}_{1c}^{-1} \mathbf{H}_{1r}^T & \mathbf{0} & \mathbf{H}_{1r} \mathbf{T}_{1c} \mathbf{D}_c \mathbf{G}_c \mathbf{D}_g^T \\ \mathbf{D}_m \mathbf{G}_c \mathbf{D}_c^T \mathbf{T}_{1c}^{-1} \mathbf{H}_{1r}^T & \mathbf{I} & \mathbf{D}_m \mathbf{G}_c \mathbf{D}_g^T \\ \mathbf{D}_g \mathbf{G}_c \mathbf{D}_c^T \mathbf{T}_{1c}^{-1} \mathbf{H}_{1r}^T & \mathbf{0} & \mathbf{G}_t + \mathbf{D}_g \mathbf{G}_c \mathbf{D}_g^T \end{bmatrix} \quad (39)$$

and the new vector of unknowns

$$\mathbf{H}_1 \mathbf{T}_1 \begin{bmatrix} \mathbf{u}_{tc} \\ \phi_{tm} \\ \mathbf{u}_{tg} \end{bmatrix} = \begin{bmatrix} \mathbf{H}_{1r} \mathbf{T}_{1c} \mathbf{u}_{tc} \\ \phi_{tm} \\ \mathbf{u}_{tg} \end{bmatrix}. \quad (40)$$

In a further step, the electrical connection of the coils will be considered by means of the interconnection matrix  $\mathbf{V}_c$ , i.e.

$$\mathbf{u}_{tc} = \mathbf{V}_c \bar{\mathbf{u}}_{tc}. \quad (41)$$

Here,  $\bar{\mathbf{u}}_{tc}$  corresponds to the independent currents of the coils. Using e.g. a wye connection of the three coils, the constraint reads as  $i_{c1} + i_{c2} + i_{c3} = 0$ , which can be accounted for by the interconnection matrix

$$\begin{bmatrix} i_{c1} \\ i_{c2} \\ i_{c3} \end{bmatrix} = \begin{bmatrix} 1 & 0 \\ 0 & 1 \\ -1 & -1 \end{bmatrix} \begin{bmatrix} i_{c1} \\ i_{c2} \end{bmatrix}. \quad (42)$$

Thus,  $\bar{\mathbf{u}}_{tc} = N_c [i_{c1}, i_{c2}]^T$  has been chosen as the vector of independent currents. Replacing  $\mathbf{u}_{tc}$  by (41) in the reduced vector of unknowns (40) results in

$$\begin{bmatrix} \mathbf{H}_{1r} \mathbf{T}_{1c} \mathbf{u}_{tc} \\ \phi_{tm} \\ \mathbf{u}_{tg} \end{bmatrix} = \begin{bmatrix} \mathbf{H}_{1r} \mathbf{T}_{1c} \mathbf{V}_c \bar{\mathbf{u}}_{tc} \\ \phi_{tm} \\ \mathbf{u}_{tg} \end{bmatrix}. \quad (43)$$

If the matrix  $\mathbf{H}_{1r} \mathbf{T}_{1c} \mathbf{V}_c$  is nonsingular,  $\bar{\mathbf{u}}_{tc}$  can be used as the new vector of independent unknown coil currents and no further action is necessary. In cases where the matrix is not square, the resulting nonlinear set of equations is overdetermined, i.e. there are more equations than unknowns. This can directly be seen by calculating the left-hand side of the reduced set of equations (38) in the form  $\mathbf{K}_3 [\bar{\mathbf{u}}_{tc}^T, \phi_{tm}^T, \mathbf{u}_{tg}^T]^T$ , with  $\mathbf{K}_3$  given by

$$\mathbf{K}_3 = \begin{bmatrix} \mathbf{S}_{11} & \mathbf{0} & \mathbf{H}_{1r} \mathbf{T}_{1c} \mathbf{D}_c \mathbf{G}_c \mathbf{D}_g^T \\ \mathbf{S}_{21} & \mathbf{I} & \mathbf{D}_m \mathbf{G}_c \mathbf{D}_g^T \\ \mathbf{S}_{31} & \mathbf{0} & \mathbf{G}_t + \mathbf{D}_g \mathbf{G}_c \mathbf{D}_g^T \end{bmatrix}, \quad (44)$$

where

$$\mathbf{S}_{11} = \mathbf{H}_{1r} \mathbf{T}_{1c} \mathbf{D}_c \mathbf{G}_c \mathbf{D}_c^T \mathbf{T}_{1c}^{-1} \mathbf{H}_{1r}^T \mathbf{H}_{1r} \mathbf{T}_{1c} \mathbf{V}_c \quad (45a)$$

$$\mathbf{S}_{21} = \mathbf{D}_m \mathbf{G}_c \mathbf{D}_c^T \mathbf{T}_{1c}^{-1} \mathbf{H}_{1r}^T \mathbf{H}_{1r} \mathbf{T}_{1c} \mathbf{V}_c \quad (45b)$$

$$\mathbf{S}_{31} = \mathbf{D}_g \mathbf{G}_c \mathbf{D}_c^T \mathbf{T}_{1c}^{-1} \mathbf{H}_{1r}^T \mathbf{H}_{1r} \mathbf{T}_{1c} \mathbf{V}_c. \quad (45c)$$

Under the previous assumption that  $\mathbf{H}_{1r} \mathbf{T}_{1c} \mathbf{V}_c$  is not square, the matrix  $\mathbf{K}_3$  has more rows than columns, which implies that not all components of the reduced flux vector  $\mathbf{H}_{1r} \mathbf{T}_{1c} \phi_{tc}$  in (38) can be arbitrarily assigned and therefore used as state variables in (21). Thus, a part of the reduced flux vector has to be added to the vector of unknowns. Let us assume that the upper-left entry  $\mathbf{S}_{11}$  of  $\mathbf{K}_3$  has  $n^\perp$  dependent rows. The transformation  $\mathbf{T}_2 = [\mathbf{S}_{11}^\perp, \mathbf{S}_{11}^I]$ , where  $\mathbf{S}_{11}^I$  is the column space of  $\mathbf{S}_{11}$  and  $\mathbf{S}_{11}^\perp$  is the orthogonal complement to  $\mathbf{S}_{11}^I$ , is used to introduce a transformed vector  $\tilde{\phi}_{tc}$  in the form

$$\mathbf{T}_2 \tilde{\phi}_{tc} = \begin{pmatrix} \mathbf{S}_{11}^\perp [\mathbf{I}, \mathbf{0}] + \mathbf{S}_{11}^I [\mathbf{0}, \mathbf{I}] \\ \mathbf{H}_{3r} & \mathbf{H}_{4r} \end{pmatrix} \tilde{\phi}_{tc} = \mathbf{H}_{1r} \mathbf{T}_{1c} \phi_{tc}. \quad (46)$$

It can be seen that adding the first  $n^\perp$  elements of  $\tilde{\phi}_{tc}$  to the vector of unknowns results in a set of nonlinear equations with a unique solution. To do so, (46) is inserted into (38) with (41) and (44), (45) resulting in

$$[\mathbf{S}_2 \quad \mathbf{K}_3] \begin{bmatrix} \mathbf{H}_{3r} \tilde{\phi}_{tc} \\ \bar{\mathbf{u}}_{tc} \\ \phi_{tm} \\ \mathbf{u}_{tg} \end{bmatrix} = - \begin{bmatrix} \mathbf{S}_{11}^I \mathbf{H}_{4r} \tilde{\phi}_{tc} \\ \mathbf{0} \\ \mathbf{0} \end{bmatrix} - \mathbf{H}_1 \mathbf{T}_1 \mathbf{M}_2, \quad (47)$$

with  $\mathbf{S}_2 = [(\mathbf{S}_{11}^\perp)^T, \mathbf{0}, \mathbf{0}]^T$ . Obviously,  $\mathbf{H}_{3r} \tilde{\phi}_{tc}$  is obtained as a solution of (47) and  $\mathbf{H}_{4r} \tilde{\phi}_{tc}$  has to be used as independent state in the dynamical equation (see (21), (38) and (41))

$$\frac{d}{dt} \mathbf{H}_{4r} \tilde{\phi}_{tc} = \mathbf{H}_{4r} \mathbf{T}_2^{-1} \mathbf{H}_{1r} \mathbf{T}_{1c} \mathbf{N}_c^{-1} (\mathbf{R}_c \mathbf{N}_c^{-1} \mathbf{V}_c \bar{\mathbf{u}}_{tc} - \mathbf{v}_c). \quad (48)$$

As a result of this modeling framework we get the DAE system (47), (48) which is of minimal dimension and systematically accounts for the electric interconnection of the coils.

### E. Simulation results

To evaluate the behavior of the PSM, simulations of the mathematical model were performed. In a first step, the torque and the magnetomotive forces for fixed currents were investigated using (18) and (20). Fig. 4(a) shows the cogging torque, i.e. the torque for zero currents  $i_{cj} = 0$ ,  $j = 1, 2, 3$ . It can be seen that a pronounced cogging torque with a periodicity of  $15^\circ$  is present in the motor. The results given in Fig. 2(b)-(d) were obtained for  $-i_{c2} = i_{c3} = 2.5$  A,  $i_{c1} = 0$  A, which approximately corresponds to the nominal value. A closer look at the torque in Fig. 4(b) shows that the characteristics of the torque is far from being sinusoidal, which would be expected for an ideal PSM. The magnetomotive forces in the stator teeth and yoke depicted in Fig. 4(c)-(d) further reveal that the magnetomotive forces in the yoke are much smaller than for the teeth.

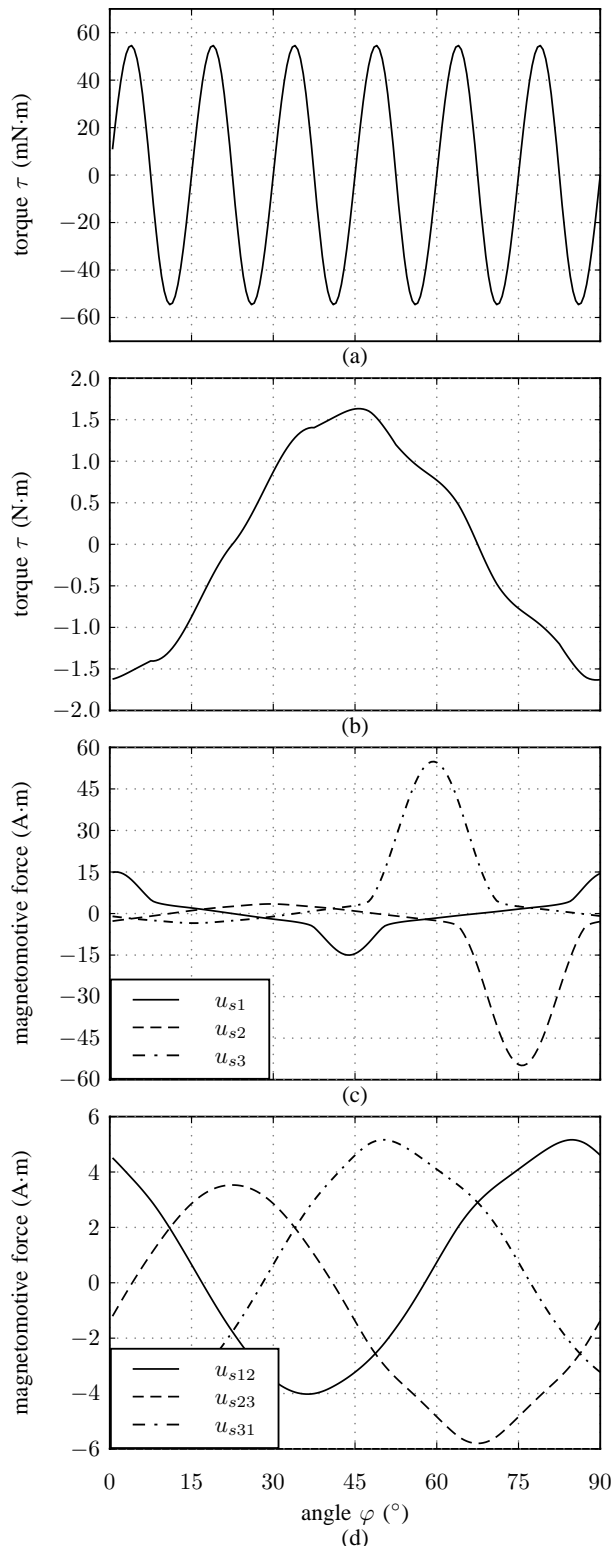


Fig. 4. Simulation results of the complete model (a) for zero currents and (b)-(d) for  $-i_{c2} = i_{c3} = 2.5$  A,  $i_{c1} = 0$  A.

This fact gives rise to the development of a simplified permeance network, which covers the essential effects of the complete model. A simplified model of reduced dimension and complexity is especially desirable for a prospective controller design. Thus, the following simplifications will be made: (i) The permeances  $G_{s12}$ ,  $G_{s23}$  and  $G_{s31}$  of the stator yoke are neglected, i.e. set to  $\infty$ . (ii) Simulations show that the fluxes in the radial rotor bars are very small compared to the fluxes in the rest of the motor. Thus, the simplification  $G_{b1} = G_{b2} = 0$  is used. (iii) With the last simplification, the circumferential rotor bars and the centre of the rotor can be modeled by a single equivalent permeance  $G_b$  and  $G_r$ , respectively.

In the subsequent section, the simplified model will be presented in more detail. A comparison of simulation results of the complete with the reduced model will justify the simplifying assumptions being made.

### III. REDUCED MODEL

#### A. Permeance network

Fig. 5 shows the reduced permeance network. Therein, the effective permeances of the circumferential bars and the center of the rotor are given by

$$G_b = \frac{A_{bc}\mu_0\mu_r \left(\frac{|u_b|}{2l_{bc}}\right)}{l_{bc}} \quad (49a)$$

$$G_r = \frac{A_r\mu_0\mu_r \left(\frac{|u_r|}{2l_r}\right)}{l_r}, \quad (49b)$$

while all other components remain the same as for the complete model.

Given the tree in Fig. 5, the flux vector of the tree permeances  $\phi_{tg}$  reads as

$$\phi_{tg} = [\phi_{s1}, \phi_{s2}, \phi_{s3}, \phi_b, \phi_{m1}, \phi_{m2}, \phi_{a11}]^T \quad (50)$$

and the vector of the co-tree fluxes is given by

$$\phi_c = [\phi_r, \phi_{l12}, \phi_{l23}, \phi_{l31}, \phi_{a12}, \phi_{a21}, \phi_{a22}, \phi_{a31}, \phi_{a32}]^T. \quad (51)$$

The magnetomotive forces are defined accordingly and the remaining fluxes and magnetomotive forces are equal to the complete model. The permeance matrices of the tree and co-tree reduce to

$$\mathbf{G}_t = \text{diag} [G_{s1}, G_{s2}, G_{s3}, G_b, G_{m1}, G_{m2}, G_{a11}] \quad (52a)$$

$$\mathbf{G}_c = \text{diag} [G_r, G_{l12}, G_{l23}, G_{l31}, G_{a12}, G_{a21}, G_{a22}, G_{a31}, G_{a32}] \quad (52b)$$

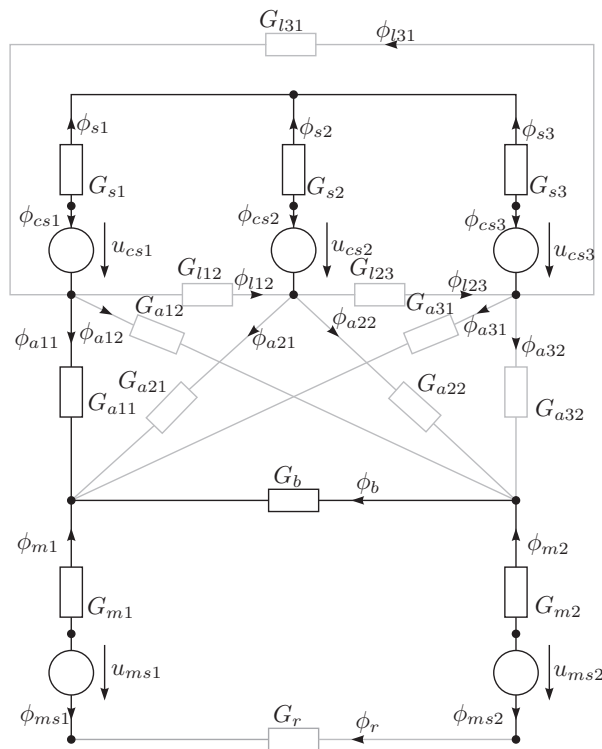


Fig. 5. Reduced permeance network of the PSM.

and the components of the incidence matrix read as

$$\mathbf{D}_c = \begin{bmatrix} 0 & 1 & 0 & -1 & 0 & -1 & -1 & -1 & -1 \\ 0 & -1 & 1 & 0 & 0 & 1 & 1 & 0 & 0 \\ 0 & 0 & -1 & 1 & 0 & 0 & 0 & 1 & 1 \end{bmatrix} \quad (53a)$$

$$\mathbf{D}_m = \begin{bmatrix} -1 & 0 & 0 & 0 & 0 & 0 & 0 & 0 & 0 \\ 1 & 0 & 0 & 0 & 0 & 0 & 0 & 0 & 0 \end{bmatrix} \quad (53b)$$

$$\mathbf{D}_g = \begin{bmatrix} 0 & -1 & 0 & 1 & 0 & 1 & 1 & 1 & 1 \\ 0 & 1 & -1 & 0 & 0 & -1 & -1 & 0 & 0 \\ 0 & 0 & 1 & -1 & 0 & 0 & 0 & -1 & -1 \\ -1 & 0 & 0 & 0 & 1 & 0 & 1 & 0 & 1 \\ 1 & 0 & 0 & 0 & 0 & 0 & 0 & 0 & 0 \\ -1 & 0 & 0 & 0 & 0 & 0 & 0 & 0 & 0 \\ 0 & 0 & 0 & 0 & -1 & -1 & -1 & -1 & -1 \end{bmatrix}. \quad (53c)$$

The balance and the torque equations are defined equally to the complete model and are, therefore, not repeated here. In the subsequent section, however, the derivation of the voltage equations according to Section II-D is carried out for the reduced model.

### B. Voltage equation

Following (22) the vector of unknowns  $\mathbf{x}$  and the right-hand side  $\mathbf{M}_1$  for the reduced permeance network of 5 are given

by

$$\mathbf{x} = [u_{cs1}, u_{cs2}, u_{cs3}, \phi_{ms1}, \phi_{ms2}, u_{s1}, u_{s2}, u_{s3}, u_b, u_{m1}, u_{m2}, u_{a11}]^T \quad (54a)$$

$$\mathbf{M}_1 = [\phi_{cs1}, \phi_{cs2}, \phi_{cs3}, 0, 0, 0, 0, 0, 0, 0, 0, 0]^T. \quad (54b)$$

The column space  $\mathbf{D}_c^I$  of  $\mathbf{D}_c$  from (53a) reads as

$$\mathbf{D}_c^I = \begin{bmatrix} 1 & 0 \\ 0 & 1 \\ -1 & -1 \end{bmatrix} \quad (55)$$

with the orthogonal complement  $\mathbf{D}_c^\perp = [1, 1, 1]^T$ . Thus, the transformation matrix  $\mathbf{T}_{1c}$  according to (24) is given by

$$\mathbf{T}_{1c} = \begin{bmatrix} 1 & 1 & 1 \\ 1 & 0 & -1 \\ 0 & 1 & -1 \end{bmatrix}, \quad (56)$$

and the matrix  $\mathbf{H}_{1r}$ , see (37) reads as

$$\mathbf{H}_{1r} = \begin{bmatrix} 0 & 1 & 0 \\ 0 & 0 & 1 \end{bmatrix}. \quad (57)$$

The linear combination of coil currents which can be calculated from the set of equations are defined by

$$\mathbf{H}_{1r} \mathbf{T}_{1c} \mathbf{u}_{tc} = \begin{bmatrix} u_{cs1} - u_{cs3} \\ u_{cs2} - u_{cs3} \end{bmatrix} \quad (58)$$

and the sum of the currents  $(\mathbf{D}_c^\perp)^T \mathbf{u}_{tc} = u_{cs1} + u_{cs2} + u_{cs3}$ , see (36), cannot be deduced from the permeance network. This is immediately clear, since applying the same current to all three coils does not change the fluxes in the machine.

The vector of independent coil fluxes is then given by

$$\mathbf{H}_{1r} \mathbf{T}_{1c} \phi_{tc} = \begin{bmatrix} \phi_{cs1} - \phi_{cs3} \\ \phi_{cs2} - \phi_{cs3} \end{bmatrix} \quad (59)$$

and the constraint  $(\mathbf{D}_c^\perp)^T \phi_{tc} = \phi_{cs1} + \phi_{cs2} + \phi_{cs3} = 0$  has to be met.

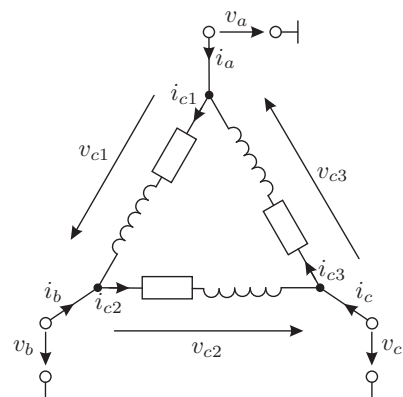


Fig. 6. Electrical connection of the motor coils (delta).

The coils of the motor are connected in delta connection, see Fig. 6, which does not directly imply an additional constraint

on the currents. The electric voltages, however, have to meet  $v_{c1} + v_{c2} + v_{c3} = 0$ . Using this constraint in the ode

$$N_c \frac{d}{dt} (\phi_{cs1} + \phi_{cs2} + \phi_{cs3}) = -R_c (i_{c1} + i_{c2} + i_{c3}) + v_{c1} + v_{c2} + v_{c3}, \quad (60)$$

$i_{c1} + i_{c2} + i_{c3} = 0$  can be directly deduced. Finally, the set of independent differential equations is given by

$$N_c \frac{d}{dt} (\phi_{cs1} - \phi_{cs3}) = -R_c (i_{c1} - i_{c3}) + v_{c1} - v_{c3} \quad (61a)$$

$$N_c \frac{d}{dt} (\phi_{cs2} - \phi_{cs3}) = -R_c (i_{c2} - i_{c3}) + v_{c2} - v_{c3}. \quad (61b)$$

*Remark 2:* Note that the electrical interconnection of the coils does not have to be considered since  $\mathbf{H}_{1r} \mathbf{T}_{1c} \mathbf{V}_c = \mathbf{I}$ , with

$$\mathbf{V}_c = \frac{1}{3} \begin{bmatrix} 2 & -1 \\ -1 & 2 \\ -1 & -1 \end{bmatrix} \quad (62)$$

and  $\bar{\mathbf{u}}_{tc} = N_c [i_{c1} - i_{c3}, i_{c2} - i_{c3}]^T$ .

### C. Comparison with complete model and measurements

To prove that the reduced model captures the essential behavior of the complete model with sufficient accuracy, a comparison of the torques for zero current (see Fig. 7(a)) and for  $-i_{c2} = i_{c3} = 2.5$  A,  $i_{c1} = 0$  A (see Fig. 7(b)) is given. It can be seen that almost perfect agreement between the two models can be achieved. The comparison of the magnetomotive force  $u_{s3}$  in Fig.7(c) shows some minor differences between the complete and reduced model, which, however, do not significantly influence the torque. Therefore, the simplifications of the reduced model can be considered feasible.

For the evaluation of the model quality in comparison with the behavior of the real motor, measurements at a test bench were performed. The test bench given in Fig. 8 is composed of (i) the PSM, (ii) a torque measurement shaft, (iii) a highly accurate resolver, (iv) an inertia disk and (v) a harmonic drive. The PSM is connected to a voltage source, where the terminal voltage  $v_c$  is adjusted to obtain a desired current  $i_c$  while the terminal voltages  $v_a$  and  $v_b$  are set to zero, see Fig. 6. To measure the torque  $\tau$  as a function of the angle  $\varphi$ , the PSM is driven by a harmonic drive motor at a constant rotational speed of  $n = 2$  rpm.

Fig. 9 depicts a comparison of the measured and simulated torque of the PSM. It can be seen that a rather good agreement between measurement and reduced model is given, which is remarkable, since the model has only been parameterized by means of geometrical and nominal material parameters.

The reduced model, however, is not accurate enough for a high precision control strategy. Therefore, the next section is concerned with the calibration of certain model parameters to further improve the model accuracy.

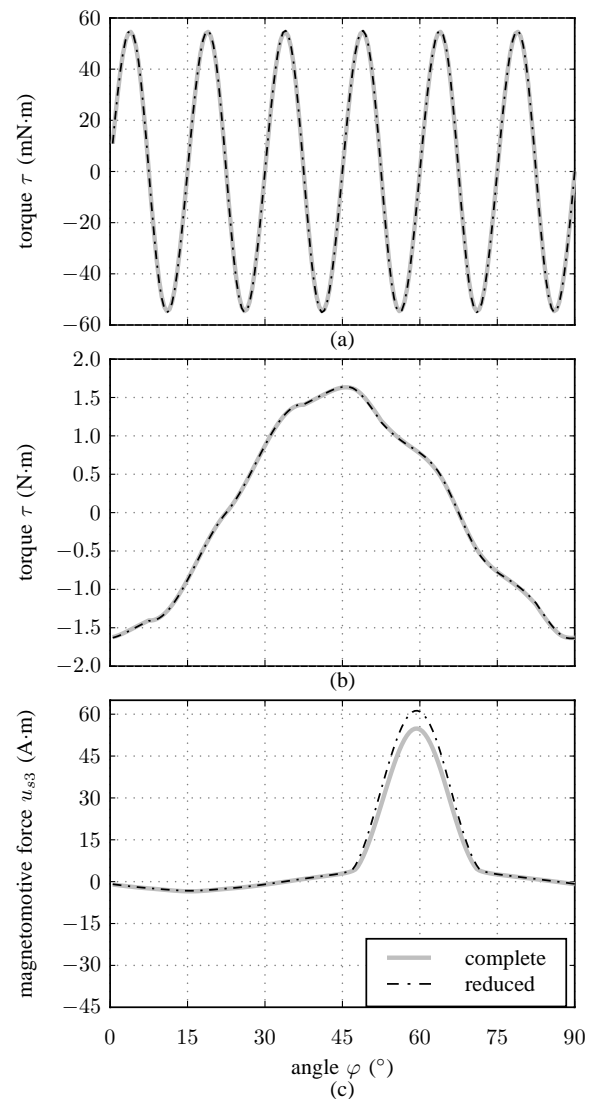


Fig. 7. Comparison of the complete with the reduced model (a) for zero currents and (b)-(c) for  $-i_{c2} = i_{c3} = 2.5$  A,  $i_{c1} = 0$  A.

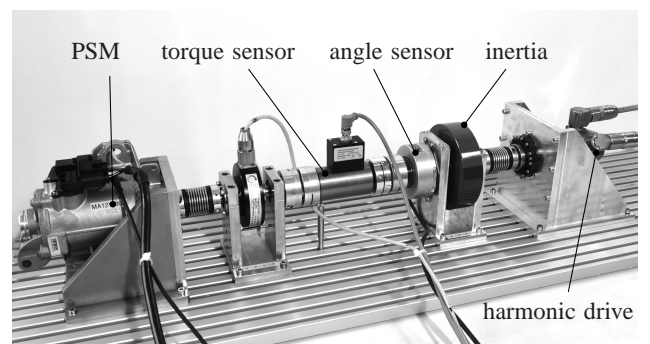


Fig. 8. Test bench for the PSM.

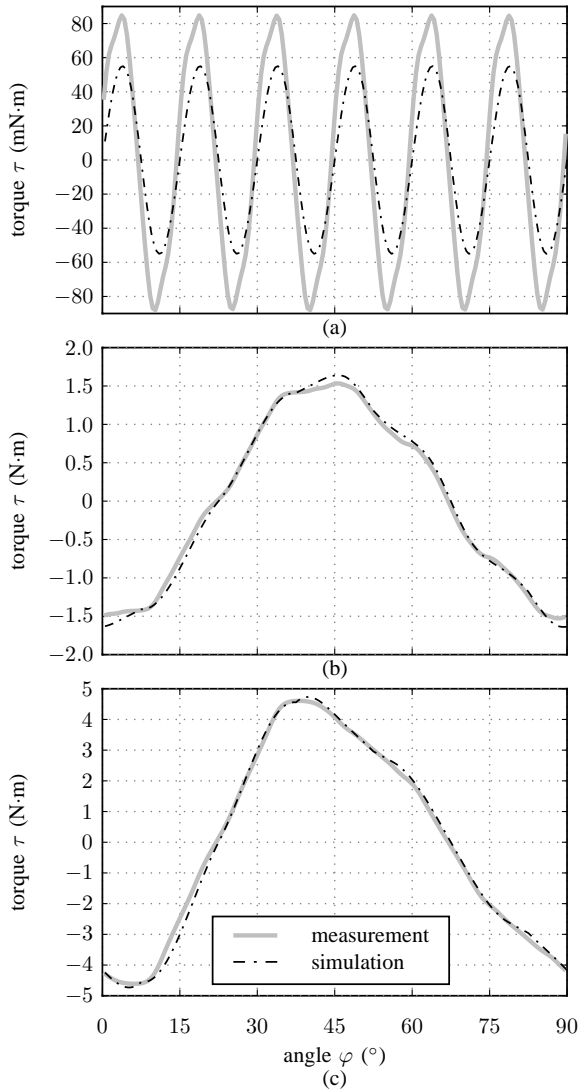


Fig. 9. Comparison of the reduced model with measurements (a) for zero currents, (b) for  $-i_{c2} = i_{c3} = 2.5$  A,  $i_{c1} = 0$  A and (c) for  $-i_{c2} = i_{c3} = 7.5$  A,  $i_{c1} = 0$  A.

#### IV. MODEL CALIBRATION

The main reason for the model errors are the inaccuracies in the air gap permeances  $G_{ajk}$ . Thus, the following strategy is introduced for the identification of the air gap permeances:

(i) The torque is measured for fixed currents  $i_{cs1} = 0$ ,  $-i_{cs2} = i_{cs3} = i_{cs}$  and a fixed step size in the angle  $\Delta\varphi$ , resulting in a measurement vector  $\tau_m^k$ ,  $k = 1, \dots, N_\varphi$  with the corresponding angles  $\varphi^k = k\Delta\varphi$ , the number of measurements  $N_\varphi$  and  $\Delta\varphi N_\varphi = \pi/2$ .

(ii) It is assumed that  $G_a = G_{a,nom} + \Delta G_a$ , with the nominal value  $G_{a,nom}$  and the corrective term  $\Delta G_a$  to be identified. Of course, the corrective term has to meet the symmetry condition (8),  $\Delta G_{alm} = \Delta G_a(\varphi - (l-1)\pi/6 - (m-1)\pi/4)$ ,  $l = 1, 2, 3$  and  $m = 1, 2$ . For fixed angles  $\varphi^k$  the corresponding values are given by  $\Delta G_{alm}^{\gamma_{lm}}$ , where the index  $\gamma_{lm}$  is defined

as

$$\gamma_{lm} = \text{mod} \left( k - (l-1) \frac{N_\varphi}{3} - (m-1) \frac{N_\varphi}{2} - 1, N_\varphi \right) + 1. \quad (63)$$

(iii) For each angle  $\varphi^k$ , the relation

$$(\mathbf{G}_t + \mathbf{D}_g \mathbf{G}_c \mathbf{D}_g^T) \mathbf{u}_{tg}^k = -\mathbf{D}_g \mathbf{G}_c (\mathbf{D}_c^T \mathbf{u}_{tc} + \mathbf{D}_m^T \mathbf{u}_{tm}) \quad (64)$$

with  $\mathbf{G}_t(\varphi^k, \mathbf{u}_{tg}^k)$  and  $\mathbf{G}_c(\varphi^k, \mathbf{u}_{tg}^k)$  has to be fulfilled, see (18).

(iv) The derivation  $\partial \Delta G_a / \partial \varphi$ , needed for the calculation of the torque, see (20), is approximated by

$$\left. \frac{\partial \Delta G_a}{\partial \varphi} \right|_{\varphi^k + \frac{\Delta\varphi}{2}} = \frac{\Delta G_a^{k+1} - \Delta G_a^k}{\Delta\varphi}. \quad (65)$$

The corresponding magnetomotive forces of the air gap also have to be evaluated at  $\varphi^k + \Delta\varphi/2$ . Since they are calculated from (64) at the angles  $\varphi^k$ , these values are obtained by averaging the magnetomotive forces at the angles  $\varphi^k$  and  $\varphi^{k+1}$ , i.e.

$$u_{alm}|_{\varphi^k + \frac{\Delta\varphi}{2}} = \frac{u_{alm}^{k+1} + u_{alm}^k}{2}, \quad (66)$$

with  $l = 1, 2, 3$  and  $m = 1, 2$ .

With these prerequisites,  $N_\varphi$  torque equations in the form  $\tau^k = \tau_m^k$  and  $7N_\varphi$  nonlinear equations defined by (64), are given. The  $N_\varphi$  unknown values of  $\Delta G_a^k$  and the  $7N_\varphi$  unknown vectors  $\mathbf{u}_{tg}^k$  are given as the solution of this set of equations. This solution is found numerically using e.g. MATLAB and results in the desired corrective term  $\Delta G_a^k$  as a function of  $\varphi$ .

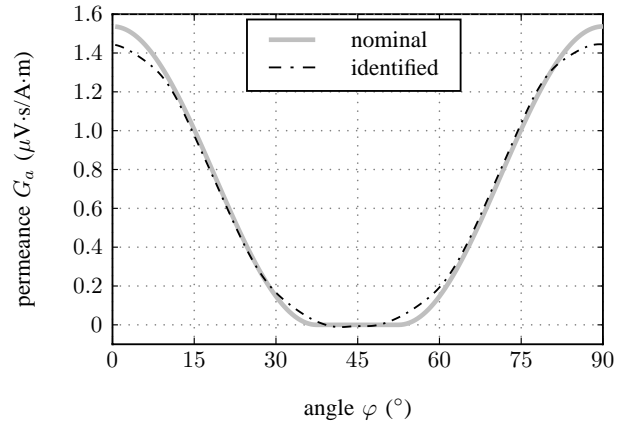


Fig. 10. Comparison of the identified and the nominal air gap permeance  $G_a(\varphi)$ .

Fig. 10 shows a comparison of the nominal air gap permeance  $G_a(\varphi)$  model adopted from [2] with the identified values, where measurements with fixed currents  $i_{cs1} = 0$ ,  $-i_{cs2} = i_{cs3} = i_{cs} = 5$  A were used for the identification. It can be seen that the basic shape is equal to the nominal characteristics, only the maximum value is reduced and the transition phase is slightly changed. The identified shape seems to be reasonable since the changes might account for unmodeled leakages.

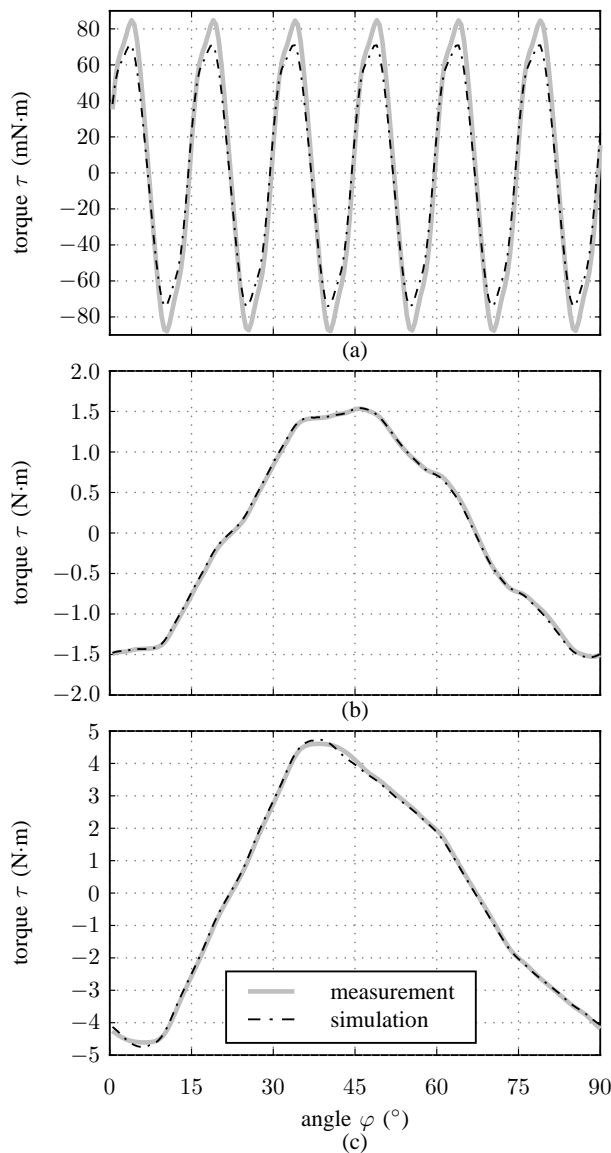


Fig. 11. Comparison of the torque of the calibrated model with measurements (a) for zero currents, (b) for  $-i_{c2} = i_{c3} = 2.5$  A,  $i_{c1} = 0$  A and (c) for  $-i_{c2} = i_{c3} = 7.5$  A,  $i_{c1} = 0$  A.

In Fig. 11, the torque of the calibrated model is compared with measurement results. These results show a significant improvement to the uncalibrated model in Fig. 9 and a very good agreement in the complete operating range of the motor. Thus, it can be deduced that both the inhomogeneous air gap as well as saturation in the motor are adequately represented by the proposed model. It is worth noting that an even better agreement between measurement and model could be achieved for the cogging torque if the calibration would have been performed at a lower current, e.g.  $i_{cs} = 2.5$  A. Then, however, the results for high currents would be worse such that the presented results are a good compromise between the accuracy for low and high currents.

The comparison of the induced voltages  $v_{csj}$ ,  $j = 1, 2, 3$  for a fixed angular velocity of 120 rad/s given in Fig. 12 further confirm the high accuracy of the proposed model.

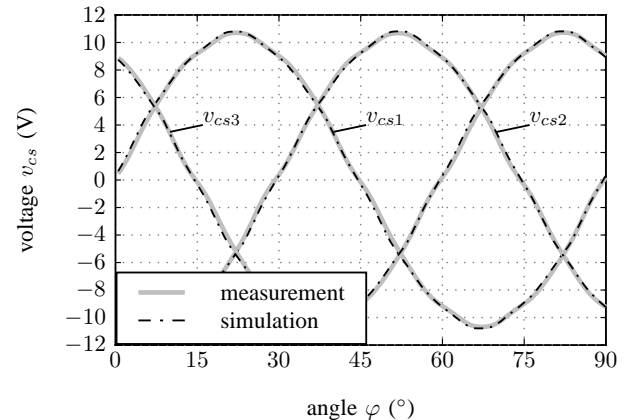


Fig. 12. Comparison of the induced voltages of the calibrated model with measurements for  $\omega = 120$  rad/s.

In conclusion, it was shown that a calibrated permeance model in form of a state-space representation with minimum number of states is suitable for the accurate description of the behavior of the motor in the complete operating range. In the subsequent section, a classical dq0-model of the motor, as it is typically employed in the controller design of PSM, will be derived. To do so, first a magnetically linear model is extracted from the nonlinear reduced model. It will be shown that the simplifications associated with the magnetically linear and especially with the dq0-model result in rather large deviations from the measurement results. This also implies that a controller design based on dq0-models is not able to exploit the full performance of model based nonlinear control strategies.

## V. SIMPLIFIED MODELS

### A. Magnetically linear model

If it is assumed that the relative permeability  $\mu_r$  of all permeances is constant, then a magnetically linear permeance model is obtained. Starting from (18) (of course using the incidence matrix  $\mathbf{D}$  and the tree and co-tree magnetomotive forces and fluxes of the reduced model of Section III), the magnetomotive forces  $\mathbf{u}_{tg}$  of the tree permeances can be calculated in the form

$$\mathbf{u}_{tg} = -(\mathbf{G}_t + \mathbf{D}_g \mathbf{G}_c \mathbf{D}_g^T)^{-1} \mathbf{D}_g \mathbf{G}_c (\mathbf{D}_c^T \mathbf{u}_{tc} + \mathbf{D}_m^T \mathbf{u}_{tm}) \quad (67)$$

and the coil fluxes  $\phi_{tc}$  read as, see (17)

$$\phi_{tc} = -\mathbf{D}_c \left[ \mathbf{G}_c - \mathbf{G}_c \mathbf{D}_g^T (\mathbf{G}_t + \mathbf{D}_g \mathbf{G}_c \mathbf{D}_g^T)^{-1} \mathbf{D}_g \mathbf{G}_c \right] (\mathbf{D}_c^T \mathbf{u}_{tc} + \mathbf{D}_m^T \mathbf{u}_{tm}). \quad (68)$$

Thus, the coil fluxes are given in the form of a superposition of the flux due to the coil currents  $\mathbf{u}_{tc} = N_c \mathbf{i}_c$  and the permanent

magnets  $\mathbf{u}_{tm}$ . Inserting (68) into the voltage equation (21), we get for the left-hand side

$$N_c \frac{d}{dt} \phi_{tc} = N_c \underbrace{\frac{\partial \phi_{tc}}{\partial \varphi}}_{\mathbf{J}} \omega + N_c \underbrace{\frac{\partial \phi_{tc}}{\partial \mathbf{i}_c}}_{\mathbf{L}} \frac{d}{dt} \mathbf{i}_c. \quad (69)$$

The (symmetric) inductance matrix  $\mathbf{L}$  can be formulated as

$$\mathbf{L} = -N_c^2 \mathbf{D}_c \left[ \mathbf{G}_c - \mathbf{G}_c \mathbf{D}_g^T (\mathbf{G}_t + \mathbf{D}_g \mathbf{G}_c \mathbf{D}_g^T)^{-1} \mathbf{D}_g \mathbf{G}_c \right] \mathbf{D}_c^T \quad (70)$$

and the vector  $\mathbf{J}$  reads as

$$\mathbf{J} = -N_c \mathbf{D}_c \mathbf{T}_J (\mathbf{D}_c^T \mathbf{u}_{tc} + \mathbf{D}_m^T \mathbf{u}_{tm}) \quad (71)$$

with

$$\mathbf{T}_J = \left[ \frac{\partial \mathbf{G}_c}{\partial \varphi} - \frac{\partial \mathbf{G}_c}{\partial \varphi} \mathbf{D}_g^T \mathbf{H}_5 \mathbf{D}_g \mathbf{G}_c - \mathbf{G}_c \mathbf{D}_g^T \mathbf{H}_5 \mathbf{D}_g \frac{\partial \mathbf{G}_c}{\partial \varphi} + \mathbf{G}_c \mathbf{D}_g^T \mathbf{H}_5 \left( \frac{\partial \mathbf{G}_t}{\partial \varphi} + \mathbf{D}_g \frac{\partial \mathbf{G}_c}{\partial \varphi} \mathbf{D}_g^T \right) \mathbf{H}_5 \mathbf{D}_g \mathbf{G}_c \right] \quad (72)$$

and

$$\mathbf{H}_5 = (\mathbf{G}_t + \mathbf{D}_g \mathbf{G}_c \mathbf{D}_g^T)^{-1}. \quad (73)$$

Given these results, the voltage equation (21) can be formulated in the well-known form

$$\mathbf{L}(\varphi) \frac{d}{dt} \mathbf{i}_c = -\mathbf{J}(\varphi) \omega + \mathbf{R}_c \mathbf{i}_c - \mathbf{v}_c. \quad (74)$$

Note that the inductance matrix  $\mathbf{L}$  and the vector  $\mathbf{J}$  are both nonlinear functions of the rotor angle  $\varphi$ . According to (20), the torque  $\tau$  of the motor in the magnetic linear case is given by

$$\tau = \underbrace{\frac{1}{2} p \mathbf{u}_{tc}^T \mathbf{D}_c \mathbf{T}_J \mathbf{D}_c^T \mathbf{u}_{tc}}_{\tau_r} + \underbrace{\frac{1}{2} p \mathbf{u}_{tm}^T \mathbf{D}_m \mathbf{T}_J \mathbf{D}_m^T \mathbf{u}_{tm}}_{\tau_c} + \underbrace{p \mathbf{u}_{tm}^T \mathbf{D}_m \mathbf{T}_J \mathbf{D}_c^T \mathbf{u}_{tc}}_{\tau_p}. \quad (75)$$

Here, three different parts can be distinguished: (i) For zero coil currents, i.e.  $\mathbf{u}_{tc} = \mathbf{0}$ , the remaining part  $\tau_c$  represents the cogging torque of the motor. (ii) Excluding the permanent magnets of the motor, i.e. setting  $\mathbf{u}_{tm} = \mathbf{0}$ , only the reluctance torque  $\tau_r$  due to the inhomogeneous air gap is present. (iii) The part  $\tau_p$  represents the main part of the torque. It is the only part which can be found in an ideal PSM with a homogenous air gap.

### B. Fundamental wave model

The magnetically linear model of the previous section still covers the complete nonlinearity due to the air gap permeances. In this subsection, a further simplification is made, where only the average values and the fundamental wave components of the corresponding parts are considered.

Applying this approach to (70), the inductance matrix is given by

$$\mathbf{L} = \begin{bmatrix} L_m & -\frac{1}{2} L_m & -\frac{1}{2} L_m \\ -\frac{1}{2} L_m & L_m & -\frac{1}{2} L_m \\ -\frac{1}{2} L_m & -\frac{1}{2} L_m & L_m \end{bmatrix}, \quad (76)$$

with the constant main inductance  $L_m$ . The term  $\mathbf{J}$  reduces to

$$\mathbf{J}(\varphi) = \hat{J} \begin{bmatrix} \sin(p\varphi) \\ \sin\left(p\varphi - \frac{2\pi}{3}\right) \\ \sin\left(p\varphi - \frac{4\pi}{3}\right) \end{bmatrix} \quad (77)$$

and the torque can be formulated as  $\tau = p \mathbf{u}_{tm}^T \mathbf{M}_{cm}(\varphi) \mathbf{u}_{tc}$ , where  $\mathbf{M}_{cm}(\varphi)$  reads as

$$\hat{M} \begin{bmatrix} \sin(p\varphi) & \sin\left(p\varphi - \frac{2\pi}{3}\right) & \sin\left(p\varphi - \frac{4\pi}{3}\right) \\ -\sin(p\varphi) & -\sin\left(p\varphi - \frac{2\pi}{3}\right) & -\sin\left(p\varphi - \frac{4\pi}{3}\right) \end{bmatrix}. \quad (78)$$

The coefficients  $L_m$ ,  $\hat{J}$  and  $\hat{M}$  can be obtained e.g. by a fourier analysis of the corresponding entries of the magnetically linear model. Fig. 13 shows a comparison of the entries of the inductance matrix  $\mathbf{L}$ , the vector  $\mathbf{J}$  and the matrix  $\mathbf{M}_{cm}$  between the magnetically linear model and the fundamental wave model. It can be seen that a rather good approximation of the magnetically linear model can be obtained by means of the fundamental wave model.

The well-known dq0-representation of the fundamental wave model can be found by using the transformations

$$\begin{bmatrix} i_d \\ i_q \\ i_0 \end{bmatrix} = \mathbf{K}(\varphi) \begin{bmatrix} i_{c1} \\ i_{c2} \\ i_{c3} \end{bmatrix}, \quad \begin{bmatrix} v_d \\ v_q \\ v_0 \end{bmatrix} = \mathbf{K}(\varphi) \begin{bmatrix} v_{c1} \\ v_{c2} \\ v_{c3} \end{bmatrix} \quad (79)$$

with the transformation matrix  $\mathbf{K}(\varphi)$ ,

$$\mathbf{K}(\varphi) = \begin{bmatrix} \cos(p\varphi) & \cos\left(p\varphi - \frac{2\pi}{3}\right) & \cos\left(p\varphi - \frac{4\pi}{3}\right) \\ \sin(p\varphi) & \sin\left(p\varphi - \frac{2\pi}{3}\right) & \sin\left(p\varphi - \frac{4\pi}{3}\right) \\ \frac{1}{2} & \frac{1}{2} & \frac{1}{2} \end{bmatrix}. \quad (80)$$

Then, the dq0-model takes the form

$$\frac{d}{dt} i_d = \frac{2}{3} \frac{1}{L_m} \left( -\frac{3}{2} L_m p \omega i_q + R_c i_d - v_d \right) \quad (81a)$$

$$\frac{d}{dt} i_q = \frac{2}{3} \frac{1}{L_m} \left( \frac{3}{2} L_m p \omega i_d - \frac{3}{2} \hat{J} \omega + R_c i_q - v_q \right) \quad (81b)$$

and the torque is given by

$$\tau = 2p \hat{M} u_{ms1} N_c i_q. \quad (82)$$

### C. Comparison of the models

Up to now three models of different complexity, i.e. a magnetically nonlinear model, a magnetically linear and a fundamental wave model, were presented in this paper. In this section, the torque  $\tau$  calculated by these models is compared with measurement results, see Fig. 14.

The results for zero current (Fig. 14(a)) show that the cogging torque can be reproduced rather well by the nonlinear model. Even the magnetically linear model shows the basic behavior of the cogging torque, however, with larger errors compared to the nonlinear model. As a matter of fact, it is not possible to reproduce the cogging torque with the fundamental wave model. Thus, this model gives the worst results as it was, of course, expected.

For nominal and high currents depicted in Fig. 14(b) and (c), respectively, this result is confirmed. Again the nonlinear model gives excellent agreement with the measurements while

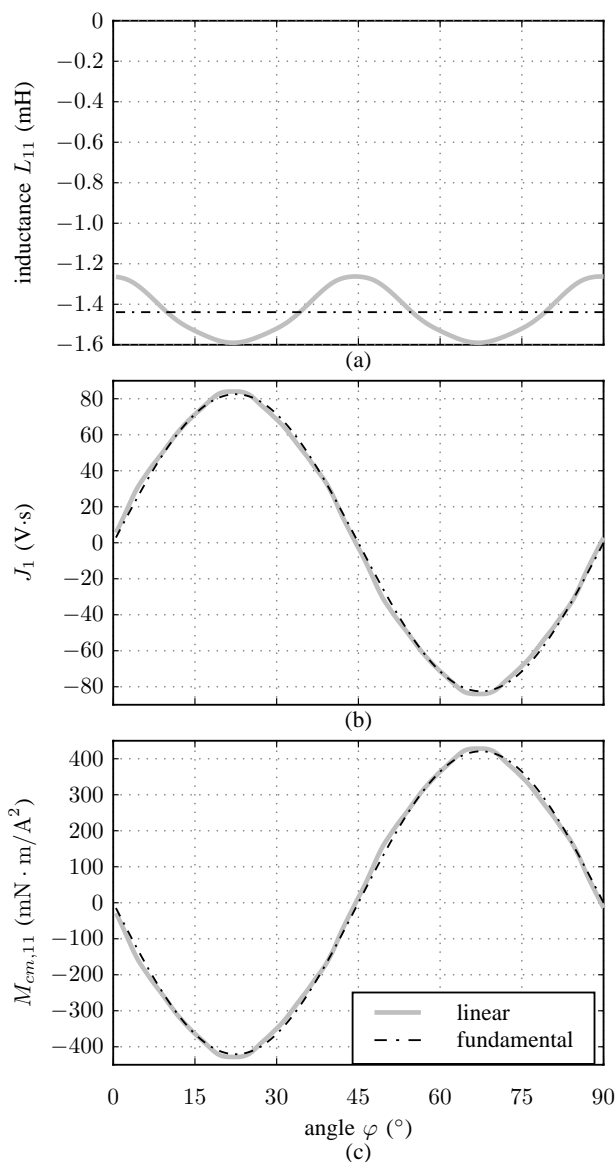


Fig. 13. (a) Entry  $L_{11}$  of the inductance matrix  $\mathbf{L}$ , (b)  $J_1$  of the vector  $\mathbf{J}$  and (c)  $M_{cm,11}$  of the matrix  $\mathbf{M}_{cm}$  for the magnetically linear and the fundamental wave model.

the performance of the magnetically linear model degrades with increasing currents. This results from the fact that saturation is not included in the magnetically linear model. The basic shape is, however, much better reproduced than in the fundamental wave model.

This brief comparison shows that a controller designed using a fundamental wave model cannot systematically account for the cogging torque and saturation. Using instead the nonlinear model for a controller design it can be expected that the control performance is superior to controllers based on fundamental wave models. The obvious drawback of the nonlinear model is the increased complexity of the resulting control strategy. Here, the magnetically linear model might

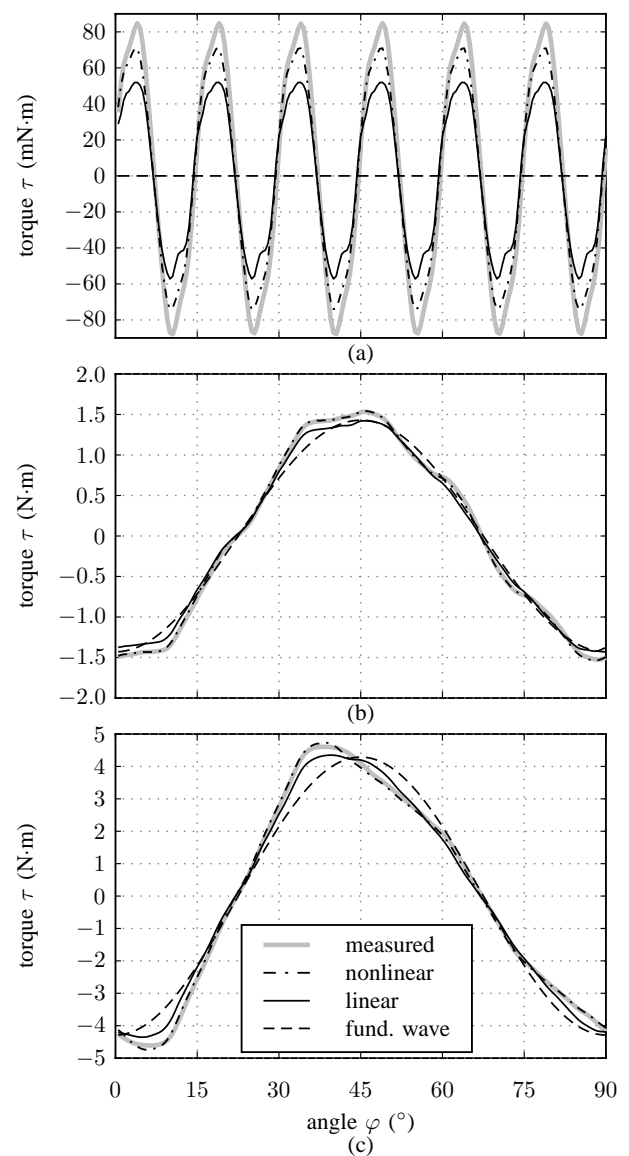


Fig. 14. Comparison of the measurement results with the nonlinear, the magnetically linear and the fundamental wave model for (a) for zero currents, (b)  $-i_{c2} = i_{c3} = 2.5$  A,  $i_{c1} = 0$  A and (c) for  $-i_{c2} = i_{c3} = 7.5$  A,  $i_{c1} = 0$  A.

be a good compromise between model complexity and model accuracy for the controller design and will yield significant improvements in comparison to fundamental wave models.

## VI. CONCLUSION

A systematic modeling framework for PSM with internal magnets was outlined in this paper. Different to existing works, the balance equations were derived based on graph-theory, which allows for a systematic calculation of the minimum number of nonlinear equations. Further, the choice of a suitable state and the systematic consideration of the electrical connection of the coils were discussed. The quality of the calibrated

model was shown by a comparison with measurement results. Finally, a magnetically linear and a dq0-model have been derived and compared with the nonlinear model.

Future work will deal with the application of the methodology to other motor designs as, e.g. PSM with surface magnets, reluctance machines or asynchronous machines. Moreover, the use of the models derived in this work for nonlinear and optimal controller design is an ongoing topic of research. Here, first results show a high potential of the modeling approach and a significant improvement in comparison to control strategies using classical dq0-models.

#### APPENDIX A EXISTENCE AND UNIQUENESS OF SOLUTION

The set of nonlinear equations in (18) has to be solved numerically. Thus, it is interesting to examine if a solution exists and if it is unique. The matrices  $\mathbf{G}_t$  and  $\mathbf{G}_c$  are positive semi-definite matrices for all  $\mathbf{u}_{tg}$  and  $\varphi$ . This can be easily seen since the entries of these diagonal matrices are positive except for the air gap permeances, which can become zero for certain angles  $\varphi$ . Moreover, a suitable construction of the permeance network ensures that  $\mathbf{D}_g$  has independent rows such that  $\mathbf{D}_g \mathbf{G}_c \mathbf{D}_g^T$  is also positive semi-definite. To show that the sum of this term with  $\mathbf{G}_t$  is even positive definite, consider the vector  $\mathbf{x}$  which fulfills

$$\mathbf{x}^T \mathbf{G}_t \mathbf{x} = 0. \quad (83)$$

The only possible solution  $\mathbf{x}$  of (83) is equal to  $\mathbf{x} = [0, \dots, \alpha]^T$ ,  $\alpha \in \mathbb{R}$ . It is then rather simple to show that

$$\mathbf{x}^T \mathbf{D}_g \mathbf{G}_c \mathbf{D}_g^T \mathbf{x} > 0, \quad \forall \mathbf{u}_{tg}, \varphi, \quad (84)$$

which implies that  $\mathbf{F} = \mathbf{G}_t + \mathbf{D}_g \mathbf{G}_c \mathbf{D}_g^T$  is positive definite. In the magnetic linear case, the permeances are independent of the magnetomotive force and therefore, the positive definiteness of  $\mathbf{F}$  is sufficient for the existence and uniqueness of a solution of (18). In the nonlinear case, however, it has to be shown the Jacobian of  $\mathbf{F}(\mathbf{u}_{tg}, \varphi) \mathbf{u}_{tg}$  is positive definite, see, e.g., [39]. The Jacobian can be written in the form

$$\mathbf{F} + \sum_{j=1}^n \frac{\partial \mathbf{F}}{\partial u_{tg,j}} \mathbf{u}_{tg}, \quad (85)$$

where  $u_{tg,j}$  describes the  $j$ -th entry of  $\mathbf{u}_{tg}$ . Using the fact that

$$\mu_r(H) + H \frac{\partial \mu_r(H)}{\partial H} > 0 \quad (86)$$

holds, it can be shown that the Jacobian (85) indeed is positive definite for all  $\mathbf{u}_{tg}$  and  $\varphi$ . It can be further shown that

$$\lim_{\|\mathbf{u}_{tg}\| \rightarrow \infty} \|\mathbf{F}(\mathbf{u}_{tg}) \mathbf{u}_{tg}\| = \infty \quad (87)$$

holds, which implies that there exists a unique solution of the set of nonlinear equations (18), see [39].

#### REFERENCES

- [1] S.-C. Yang, T. Suzuki, R. D. Lorenz, and T. M. Jahns, "Surface-permanent-magnet synchronous machine design for saliency-tracking self-sensing position estimation at zero and low speeds," *IEEE Transactions on Industry Applications*, vol. 47, pp. 2103–2116, 2011.
- [2] V. Ostovic, *Dynamics of Saturated Electric Machines*. Springer, 1989.
- [3] J. R. Hendershot and T. J. E. Miller, *Design of Brushless Permanent-Magnet Machines*. Motor Design Books LLC, 2010.
- [4] D. Hanselman, *Brushless Permanent Magnet Motor Design*. Magna Physics Publishing, 2006.
- [5] G. Y. Sizov, D. M. Ionel, and N. A. O. Demerdash, "Multi-objective optimization of pm ac machines using computationally efficient - fea and differential evolution," in *Proceedings of the International Electric Machines and Drives Conference*, 2011.
- [6] Y. Perriard, "Reluctance motor and actuator design: Finite-element model versus analytical model," *IEEE Transactions on Magnetics*, vol. 40, pp. 1905–1910, 2004.
- [7] K. Reichert, "A simplified approach to permanent magnet and reluctance motor characteristics determination by finite-element methods," *International Journal for Computation and Mathematics in Electrical and Electronic Engineering*, vol. 25, pp. 368–378, 2006.
- [8] B. Tomczuk, G. Schröder, and A. Waindok, "Finite-element analysis of the magnetic field and electromechanical parameters calculation for a slotted permanent-magnet tubular linear motor," *IEEE Transactions on Magnetics*, vol. 43, pp. 3229–3236, 2007.
- [9] D. M. Ionel and M. Popescu, "Finite-element surrogate model for electric machines with revolving field: Application to ipm motors," *IEEE Transactions on Industry Applications*, vol. 46, pp. 2424–2433, 2010.
- [10] M. A. Jabbar, H. N. Phyu, Z. Liu, and C. Bi, "Modeling and numerical simulation of a brushless permanent-magnet dc motor in dynamic conditions by time-stepping technique," *IEEE Transactions on Industry Applications*, vol. 40, pp. 763–770, 2004.
- [11] W. Leonhard, *Control of Electrical Drives*, 2nd ed. Springer, 1997.
- [12] P. C. Krause, O. Wasynczuk, and S. D. Sudhoff, *Analysis of Electric Machinery and Drive Systems*. IEEE Press, 2002.
- [13] C. Gerada, K. J. Bradley, M. Sumner, and G. Asher, "Non-linear dynamic modelling of vector controlled pm synchronous machines," in *Proceedings of the European Conference on Power Electronics and Applications*, 2005, pp. 10–P.10.
- [14] A. E. Fitzgerald, C. Kingsley, and S. D. Umans, *Electric Machinery*. McGraw-Hill, 2003.
- [15] D. M. Dawson, J. Hu, and T. C. Burg, *Nonlinear Control of Electric Machinery*. Marcel Dekker, 1998.
- [16] F. Morel, J.-M. Retif, X. Lin-Shi, and C. Valentin, "Permanent magnet synchronous machine hybrid torque control," *IEEE Transactions on Industrial Electronics*, vol. 55, pp. 501–511, 2008.
- [17] T. Geyer, G. A. Beccuti, G. Papafiotou, and M. Morari, "Model predictive direct torque control of permanent magnet synchronous motors," in *Proceedings of the Energy Conversion Congress and Exposition*, 2010, pp. 199–206.
- [18] C.-K. Lin, T.-H. Liu, and L.-C. Fu, "Adaptive backstepping pi sliding-mode control for interior permanent magnet synchronous motor drive systems," in *Proceedings of the American Control Conference*, 2011, pp. 4075–4080.
- [19] V. Ostovic, "A novel method for evaluation of transient states in saturated electric machines," *IEEE Transactions on Industrial Applications*, vol. 24, pp. 96–100, 1989.
- [20] L. Zhu, S. Z. Jiang, Z. Q. Zhu, and C. C. Chan, "Analytical modeling of open-circuit air-gap field distributions in multisegment and multilayer interior permanent-magnet machines," *IEEE Transactions on Magnetics*, vol. 45, pp. 3121–3130, 2009.
- [21] A. R. Tariq, C. E. Nino-Baron, and E. G. Strangas, "Iron and magnet losses and torque calculation of interior permanent magnet synchronous machines using magnetic equivalent circuit," *IEEE Transactions on Magnetics*, vol. 46, pp. 4073–4080, 2010.
- [22] J. Tangdu, T. Jahns, and A. El-Refai, "Core loss prediction using magnetic circuit model for fractional-slot concentrated-winding interior permanent magnet machines," in *Proceedings of the IEEE Energy Conversion Congress and Exposition*, 2010, pp. 1004–1011.
- [23] B. Sheik-Ghalavand, S. Vaez-Zadeh, and A. H. Isfahani, "An improved magnetic equivalent circuit model for iron-core linear permanent-magnet synchronous motors," *IEEE Transactions on Magnetics*, vol. 46, pp. 112–120, 2010.
- [24] S. Serri, A. Tani, and G. Serra, "A method for non-linear analysis and calculation of torque and radial forces in permanent magnet multiphase bearingless motors," in *Proceedings of the International Symposium on*

- Power Electronics, Electrical Drives, Automation and Motion*, 2012, pp. 75–82.
- [25] H. Seok-Hee, T. Jahns, and W. Soong, “A magnetic circuit model for an ipm synchronous machine incorporating moving airgap and cross-coupled saturation effects,” in *Proceedings of the IEEE International Electric Machines & Drives Conference*, 2007, pp. 21–26.
- [26] T. Raminosoa, J. Farooq, A. Djerdir, and A. Miraoui, “Reluctance network modelling of surface permanent magnet motor considering iron nonlinearities,” *Energy Conversion and Management*, vol. 50, pp. 1356–1361, 2009.
- [27] T. Raminosoa, I. Rasoanarivo, and F.-M. Sargos, “Reluctance network analysis of high power synchronous reluctance motor with saturation and iron losses considerations,” in *Proceedings of the Power Electronics and Motion Control Conference*, 2006, pp. 1052–1057.
- [28] Y. Kano, T. Kosaka, and N. Matsui, “Simple nonlinear magnetic analysis for permanent-magnet motors,” *IEEE Transactions on Industry Applications*, vol. 41, pp. 1205–1214, 2005.
- [29] A. Ibala, A. Masmoudi, G. Atkinson, and A. G. Jack, “On the modeling of a tfrm by reluctance network including the saturation effect with emphasis on the leakage fluxes,” *International Journal for Computation and Mathematics in Electrical and Electronic Engineering*, vol. 30, pp. 151–171, 2011.
- [30] M.-F. Hsieh and Y.-C. Hsu, “A generalized magnetic circuit modeling approach for design of surface permanent-magnet machines,” *IEEE Transactions on Industrial Electronics*, vol. 59, pp. 779–792, 2012.
- [31] M. Amrhein and P. T. Krein, “3-d magnetic equivalent circuit framework for modeling electromechanical devices,” *IEEE Transactions on Energy Conversion*, vol. 24, pp. 379–405, 2009.
- [32] ———, “Force calculation in 3-d magnetic equivalent circuit networks with a maxwell stress tensor,” *IEEE Transactions on Magnetics*, vol. 24, pp. 587–593, 2009.
- [33] J. D. Law, T. J. Busch, and T. A. Lipo, “Magnetic circuit modeling of the field regulated reluctance machine part i: Model development,” *IEEE Transactions on Energy Conversion*, vol. 11, pp. 49–55, 1996.
- [34] M. L. Bash, J. M. Williams, and S. D. Pekarek, “Incorporating motion in mesh-based magnetic equivalent circuits,” *IEEE Transactions on Energy Conversion*, vol. 25, pp. 329–338, 2010.
- [35] M. L. Bash and S. D. Pekarek, “Modeling of salient-pole wound-rotor synchronous machines for population-based design,” *IEEE Transactions on Energy Conversion*, vol. 26, pp. 381–392, 2011.
- [36] N. Christofides, *Graph Theory: An Algorithmic Approach*. Academic Press, 1975.
- [37] L. O. Chui, C. A. Desoer, and E. S. Kuh, *Linear and Nonlinear Circuits*. McGraw-Hill, 1987.
- [38] A. Kugi, *Non-linear Control Based on Physical Models*. Springer, 2001.
- [39] F. Wu and C. Desoer, “Global inverse function theorem,” *IEEE Transactions on Circuit Theory*, vol. 19, pp. 199–201, 1972.



**Wolfgang Kemmetmüller** (M'04) received the Dipl.-Ing. degree in mechatronics from the Johannes Kepler University Linz, Austria, in 2002 and his Ph.D. (Dr.-Ing.) degree in control engineering from Saarland University, Saarbruecken, Germany, in 2007. From 2002 to 2007 he worked as a research assistant at the Chair of System Theory and Automatic Control at Saarland University. From 2007 to 2012 he has been a senior researcher at the Automation and Control Institute at Vienna University of Technology, Vienna, Austria and since 2013 he is

Assistant Professor. His research interests include the physics based modeling and the nonlinear control of mechatronic systems with a special focus on electrohydraulic and electromechanical systems where he is involved in several industrial research projects. Dr. Kemmetmüller is associate editor of the IFAC journal *Mechatronics*.



**David Faustner** received the Dipl.-Ing. degree in electrical engineering from the Vienna University of Technology, Austria, in October 2011. Since November 2011 he works as a research assistant at the Automation and Control Institute at Vienna University of Technology. His research interests include the physics based modeling and the nonlinear control of electrical machines.



**Andreas Kugi** (M'94) received the Dipl.-Ing. degree in electrical engineering from Graz University of Technology, Austria, and the Ph.D. (Dr. techn.) degree in control engineering from Johannes Kepler University (JKU), Linz, Austria, in 1992 and 1995, respectively. From 1995 to 2000 he worked as an assistant professor and from 2000 to 2002 as an associate professor at JKU. He received his “Habilitation” degree in the field of automatic control and control theory from JKU in 2000. In 2002, he was appointed full professor at Saarland University, Saarbrücken, Germany, where he held the Chair of System Theory and Automatic Control until May 2007. Since June 2007 he is a full professor for complex dynamical systems and head of the Automation and Control Institute at Vienna University of Technology, Austria.

His research interests include the physics-based modeling and control of (nonlinear) mechatronic systems, differential geometric and algebraic methods for nonlinear control, and the controller design for infinite-dimensional systems. He is involved in several industrial research projects in the field of automotive applications, hydraulic and pneumatic servo-drives, smart structures and rolling mill applications. Prof. Kugi is Editor-in Chief of the IFAC journal *Control Engineering Practice* and since 2010 he is corresponding member of the Austrian Academy of Sciences.